

On solutions relating to conical vortices over a plane wall†

By C. SOZOU

Department of Applied and Computational Mathematics, The University, Sheffield S10 2TN, UK

(Received 8 July 1991 and in revised form 7 May 1992)

It is shown that certain similarity solutions relating to axisymmetric vortices in a viscous fluid over a plane wall can be associated with a point source or sink of vorticity at the origin and a line vortex along the symmetry axis of the system. The rotationality of the nonlinear terms in the momentum equation, due to the radial vorticity and the azimuthal flow field, induces a poloidal flow which relates to one-cell or two-cell configurations. It is shown that a small input of radial vorticity into a strong line vortex can induce an intense up-draught. There are ranges of values of the parameters yielding two solutions. The extremities of these ranges are associated with values that yield velocity breakdown.

1. Introduction

Similarity solutions relating to steady axisymmetric vortices in a viscous semi-infinite fluid bounded by a plane wall have been considered by several authors including Goldshtik (1960) and Serrin (1972). Goldshtik's solution has a singularity in the azimuthal component of the velocity field v along the symmetry axis which is caused by a line vortex. That solution relates to an inflow near the wall and an up-draught along the symmetry axis and breaks down when the parameter $k = \Gamma/2\nu$ exceeds a critical value which is about 2.765. Here $2\pi\Gamma$ is the circulation associated with the line vortex along the symmetry axis and ν the coefficient of kinematic viscosity of the fluid. The Goldshtik solution exhibits features associated with atmospheric vortices, such as tornadoes and waterspouts, but the value of k at breakdown is too small for such vortices. The solutions constructed by Serrin relate to one-cell or two-cell flows and do not have such a severe limitation on the value of k but they have a singularity along the axis of the system in both the azimuthal and axial component of v . Since there is a line vortex along the axis of the system the presence there of a singularity in v may not appear a severe difficulty but the singularity in the axial component of v is not caused by the vortex. It is inherent in the structure of the poloidal flow considered by Serrin and persists when the rotation is switched off. The singularity is compatible with a force along the axis of symmetry with density inversely proportional to the distance from the origin (Paull & Pillow 1985*a*; Goldshtik & Shtern 1990). Obviously there are problems with the setting up, let alone maintaining such a configuration.

Yih *et al.* (1982) relaxed the no-slip condition on the wall and constructed one-cell and two-cell vortex solutions such that v is finite on the axis of the system. On the wall the tangential component of v is not zero. These authors claimed that their solutions are distinct from those previously found. However, they did not put

† With an Appendix by M. A. Goldshtik and V. N. Shtern.

forward any suggestions concerning the origin of the azimuthal flow associated with the solutions they constructed.

Paull & Pillow (1985*b*) showed that in a unbounded fluid the rotation associated with the similarity solutions described here and known as conical vortices can be induced by two independent semi-infinite lines of torque producing singularities along the axis of the system.

Goldshnik suggested that the configuration he studied can be generated by the constant rotation of a thin long cylindrical rod along the symmetry axis of the system. For such an arrangement the radial velocity along the axis would be zero but this is not the case for the solution constructed. Indeed when k is close to its critical value the flow associated with his solution has a jet-like structure in the axial region.

The electrical analogy

We note that in all the above-mentioned studies the vorticity, in a spherical polar coordinate system (r, θ, ϕ) , is of the form $f(\theta)/r^2$ and its radial component is not zero, that is the origin acts like a vorticity source or sink. The radial vorticity and the azimuthal velocity correspond, respectively, to the current density \mathbf{j} and the magnetic induction \mathbf{B} associated with some magnetohydrodynamic (MHD) problems that were considered some twenty years ago by several authors including Lundquist (1969), Sozou (1971) and Shivola & Shcherbinin (1971). In appropriate units \mathbf{j} and \mathbf{B} are connected by the relationship $\nabla \times \mathbf{B} = \mathbf{j}$ and in those problems the electric current is brought by a thin wire along the line $\theta = \pi$ to the origin and is discharged radially into a conducting fluid occupying the region $\theta < \frac{1}{2}\pi$. The $\mathbf{j} \times \mathbf{B}$ or Lorentz force due to \mathbf{j} and the associated \mathbf{B} is rotational and, since it cannot be balanced by a pressure gradient, generates a poloidal flow field. By analogy, in conical vortices the azimuthal velocity can be thought of as generated by the vortex lines and, in the absence of other causes, the poloidal flow field by the rotationality of the vector product of the radial vorticity and the associated azimuthal velocity. For the MHD problem, in the case of small magnetic Reynolds numbers R_m , \mathbf{j} is independent of θ and the Lorentz force is independent of the poloidal flow it drives. In the case of small Reynolds numbers R the parameters associated with the conical vortices bounded by a plane wall have the same structure as the corresponding parameters for the MHD problem. In particular the study of Yih *et al.*, relating to the case $R \ll 1$ and (in their notation) $T = 0$, yields a radial vorticity and an azimuthal velocity field which, apart from proportionality constants, are equal to the expressions for \mathbf{j} and \mathbf{B} associated with Lundquist's study. Also for this case the poloidal flow field, apart from a negative constant factor, is the same as that found by Lundquist. When R is not small the radial vorticity is convected by the poloidal flow and its distribution is dependent on θ . The current density in the corresponding MHD problem when R_m is not small is also convected by the poloidal flow (Sozou & English 1972).

The solution constructed by Goldshnik relates to the case where the origin acts like a sink of vorticity and all the vorticity accumulated there is discharged in the axial direction in the form of a line vortex along the axis $\theta = 0$ so that the vorticity flux out of the surface $\theta < \frac{1}{2}\pi$ is zero. The vorticity configuration of this solution is compatible with suggestions, for example by Lighthill (1963), associating atmospheric vortices, such as whirlwinds, with the upward tilting of horizontal vortex tubes in the boundary layer on the ground. Figure 1 is a reproduction of Lighthill's figure II.3, p. 50 and illustrates schematically the proposed configuration. According to our ideas there is a secondary poloidal flow associated with the configuration of figure 1. A suggestion similar to that of Lighthill was put forward by Maxworthy

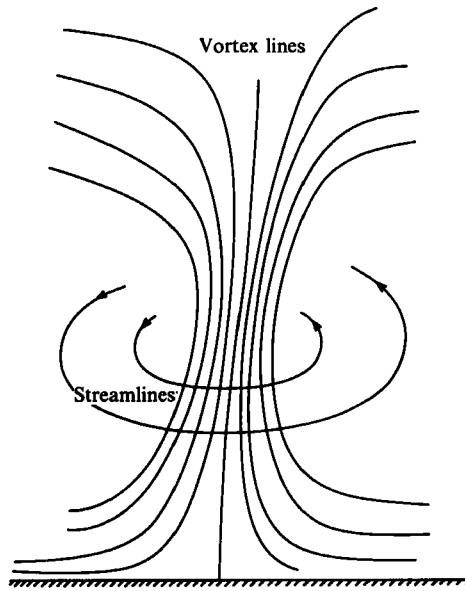


FIGURE 1. Lighthill's model for a whirlwind.

Cloud is way up above

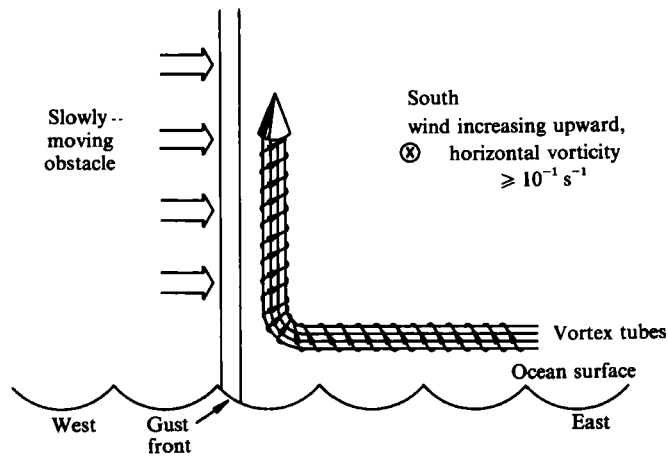


FIGURE 2. Upward tilting of vortex tubes in lowest boundary layer by gust fronts for a waterspout configuration, according to Simpson (1982, figure 5.2). The resulting whirling is postulated.

(1973), concerning the formation of dust devils. Maxworthy says also that the tilted vortex lines pass over the column of the dust devil and descend to the ground at a distant location and do not interact with the basic vortex.

A similar mechanism was invoked by Simpson (1982) concerning the generation of waterspouts, that is intense columnar vortices over water. Figure 2 is a reproduction of Simpson's figure 5.2 and illustrates schematically the proposed configuration. She points out (p. 170) that a gust front is a wedge of cold dense air which is assumed to tip bundles of horizontal vortex tubes vertically upwards and thus induces circulation around the tilted bundle. It is generally believed that in such configurations there

occurs intensification of the axial vorticity by the stretching over a relatively short time of the vertical part of the vortex tubes. For example, Simpson *et al.* (1986) estimated (p. 773) that in waterspouts the vertical vorticity, due to stretching, can increase by a factor of 20 in five minutes.

Also, according to Snow (1984), convergence of background vorticity, tilting and vertical stretching are the processes that lead to the formation of tornado vortices.

The stretching of the axial vorticity, for the simplified idealized configuration considered here, is represented by an intensified line vortex along the axis of the system, so that there is a net vorticity flux out of the surface $\theta < \frac{1}{2}\pi$, which means that the condition of zero azimuthal velocity on the wall $\theta = \frac{1}{2}\pi$ is not satisfied. Here we investigate mainly such configurations assuming the flow is driven by radial vorticity. When the vorticity input is stopped the vortex, due to diffusion, dissipates. The atmospheric vortices are complex phenomena and the simple similarity solutions presented below cannot provide quantitative information concerning the processes associated with these vortices. However, they support the view that the stretching of the axial vorticity results in the intensification of the flow that is induced by converging vorticity and are compatible with values of $k \geq 2.7$ at the breakdown stage.

2. General equations

The general equations of the problem have been derived by several authors, including Serrin and Goldshtik & Shtern, and their details will not be repeated here. Below we briefly summarize the main features of the equations.

Let p, ρ, ν and \mathbf{v} denote the pressure, density, coefficient of kinematic viscosity and velocity of an incompressible viscous fluid which is bounded by the plane $\theta = \frac{1}{2}\pi$ of a spherical polar coordinate system (r, θ, ϕ) . The line $\theta = 0$ is along the axis of symmetry of the system and is directed into the fluid. The velocity is assumed to be steady axisymmetric and to be given by

$$\mathbf{v} = (1/r) [-\nu g', -\nu g/(1-\mu^2)^{\frac{1}{2}}, \Gamma\Omega/(1-\mu^2)^{\frac{1}{2}}], \tag{1}$$

where $\mu = \cos \theta$, Γ is a constant that has the dimensions of circulation, g and Ω are functions of μ and a prime denotes differentiation with respect to μ . The wall $\theta = \frac{1}{2}\pi$ bounding the system corresponds to $\mu = 0$ and the axis of the system to $\mu = 1$. The function $g(\mu)$ can be related to a stream function ψ such that

$$\psi = \nu r g(\mu). \tag{2}$$

The fluid vorticity $\zeta = \nabla \times \mathbf{v}$ turns out to be

$$\zeta = -(1/r^2) [\Gamma\Omega', 0, \nu(1-\mu^2)^{\frac{1}{2}}g'']. \tag{3}$$

The ϕ -component and the curl of the momentum equation yield, respectively,

$$(1-\mu^2)\Omega'' - g\Omega' = 0, \tag{4}$$

$$gg''' + 3g'g'' - (1-\mu^2)g^{iv} + 4\mu g''' = 2k^2G''', \tag{5}$$

where

$$G''' = -4\Omega\Omega'/(1-\mu^2) \tag{6}$$

and $k = \Gamma/2\nu$. Integrating (5) three times and adjusting the constants of integration we obtain

$$g^2 - 2(1-\mu^2)g' - 4\mu g = 4k^2G(\mu), \tag{7}$$

where

$$G(\mu) = 2(1-\mu^2)^2 \int_0^\mu \frac{t\Omega^2(t) dt}{(1-t^2)^2} + 2\mu \int_\mu^1 \frac{\Omega^2(t) dt}{(1+t)^2} + P\mu^2 + Q\mu + S, \tag{8}$$

and P , Q are S and constants.

If we set

$$g = -2(1 - \mu^2) u' / u, \quad (9)$$

(4) and (7) become

$$u\Omega'' + 2u'\Omega' = 0, \quad (10)$$

$$u'' = k^2 Gu / (1 - \mu^2)^2. \quad (11)$$

Integrating (10) twice we obtain

$$\Omega = a + b - b \int_0^\mu u^{-2}(t) dt \Big/ \int_0^1 u^{-2}(t) dt, \quad (12)$$

where $a = \Omega(1)$ and $b = \Omega(0) - \Omega(1)$. Note that if the terms a and $a + b$ have the same sign, then Ω does not change sign.

The component of the azimuthal velocity v_ϕ associated with the term a in (12) represents the flow due to a line vortex along the axis of symmetry of the system with circulation $2\pi a\Gamma$. The component of v_ϕ associated with the constant b in (12) represents the flow induced by a vorticity source at the origin of strength b , such that the vorticity flux out of the hemispherical surface S_0 , $0 \leq \theta < \frac{1}{2}\pi$, is $2\pi b\Gamma$. (In the special case $u \approx 1$ (see (14) and (15) later) the vorticity source is isotropic, that is $r \cdot \zeta = \Gamma b/r$.) Thus the total flux of the vorticity ζ out of S_0 is $2\pi(a + b)\Gamma$. If $b < 0$ and $a + b = 0$ the radial vorticity converges to the origin and is discharged in the form of a line vortex along the axis of the system. If the line vortex undergoes intensification then $a > -b$ and (see (12)) $\Omega(0) > 0$.

3. Boundary conditions

Since g is proportional to u'/u (see (9)), without loss of generality, we can set $u(0) = 1$. The condition that the normal velocity is zero on the plane $\mu = 0$ yields $g(0) = 0$, that is $u'(0) = 0$. If $u(\mu) = 0$ at some μ , $g(\mu)$ and $g'(\mu)$ are infinite there and we have velocity breakdown. Thus (11) must be solved subject to $u(0) = 1$, $u'(0) = 0$, $u(\mu) > 0$. The constants a , b , P , Q and S are specified by the boundary conditions concerning the behaviour of v on the wall and the axis of the system. In general, not all conditions can be satisfied and a variety of conditions have been used by different authors.

The special case $\Omega = 0$ was investigated by Squire (1952) who imposed the condition of finite velocity on the axis $\mu = 1$. This condition requires (see (1)) that $g(1) = 0$, $g'(1) = \text{finite}$ and implies $G(1) = G'(1) = 0$, that is $Q = -2P$, $S = P$. The condition of zero radial velocity on the wall, that is $g'(0) = 0$, cannot be satisfied and was disregarded. For such a configuration there is an analytic one-cell solution (for details see Squire 1952) valid for $k^2P > -3.84$, except $P = 0$. The case $P < 0$ relates to inflow near the wall and up-draught in the axial region and the case $P > 0$ relates to the opposite picture.

Yih *et al.* investigated the interaction of the Squire solution in the presence of a point source of vorticity such that $a = 0$, $b = 1$, that is $\Omega(0) = 1$, $\Omega(1) = 0$. The velocity fields associated with the solutions of Yih *et al.* are finite, except at the origin, but their azimuthal and (in general) radial components are not zero on the wall $\mu = 0$.

If, again for the special case $\Omega = 0$, we set $v = 0$ on the wall and $\psi = 0$ on the symmetry axis then $g(0) = 0$, $g'(0) = 0$, $g(1) = 0$. These conditions require that $G(0) = G(1) = 0$, and yield $G = P(\mu^2 - \mu)$. It can be shown computationally that for

this form of G the solution of (11) yields a velocity field such that $u > 0$ in $0 < \mu < 1$ for $k^2P < 7.644 = A_0$. The poloidal flow is a one-cell regime, which for $P > 0$ relates to a central up-draught and for $P < 0$ relates to a central down-draught. The maximum value of $k^2P = A_0$ is associated with the limiting case $u(1) = 0$ and was also obtained by Goldshtik & Shtern. The radial velocity is $-vg'(\mu)/r$ and it can be shown that for the boundary conditions mentioned here g' has a logarithmic singularity at $\mu = 1$. This singularity is the price, in comparison with the Squire solution, for satisfying the condition $v = 0$ on the wall $\mu = 0$. It was shown by Paull & Pillow (1985a) and by Goldshtik & Shtern that the logarithmic singularity in $g'(\mu)$ on the axis of the system is associated with a force along this axis with density inversely proportional to the distance from the origin. This configuration (with the logarithmic singularity) was studied by Serrin in the presence of a point sink of vorticity at the origin with the vorticity of the sink being discharged in the form of a line vortex along the symmetry axis such that $a = 1$, $b = -1$ and so $\Omega(0) = 0$, $\Omega(1) = 1$. The special case $a = -b = P = 1$ is that studied by Goldshtik and yields $g'(1) = \text{finite}$ and has no line force along the axis $\mu = 1$.

The quantity Ω is given by (12) and if there is vorticity flux out of the surface $\theta < \frac{1}{2}\pi$, then $\Omega(0) \neq 0$. Here we assume that the non-azimuthal component of v is zero on the wall $\mu = 0$ and finite on the axis $\mu = 1$. These conditions require that $g(0) = 0 = g'(0) = g(1)$, $g'(1) = \text{finite}$. Scrutiny of (7), (8) and (12) shows that the conditions imposed on the g -function require that $G(0) = G(1) = G'(1) = 0$, that is $P = -Q = a^2$, $S = 0$. Hence

$$G(\mu) = 2(1-\mu)^2 \int_0^\mu \frac{t(\Omega^2(t) - a^2)}{(1-t^2)^2} dt + 2\mu \int_\mu^1 \frac{\Omega^2(t) - a^2}{(1+t)^2} dt. \quad (13)$$

Thus for specified a and b we must solve (11), (12) and (13) subject to $u(0) = 1$, $u'(0) = 0$ and $u > 0$.

If $b = 0$, $\Omega = a$ (from (12)), and then $G = 0$, $u = 1$ and $g = 0$, that is the g -field is driven by the vorticity source. In effect the g -field is generated by the rotationality of the $\zeta \times v$ term in the momentum equation (due to the radial vorticity and the associated azimuthal flow) that cannot be balanced by a pressure gradient. The same type of situation arises in a similar problem concerning the magneto-hydrodynamics of an electric current discharged from a point in a semi-infinite fluid (Lundquist 1969; Sozou 1971; Sozou & English 1972). In that case the electric current density corresponds to the radial vorticity. It induces the magnetic induction field which corresponds to the azimuthal velocity. The flow is poloidal and is generated by the rotationality of the Lorentz force due to the electric current density and the associated magnetic induction. Equations (4) and (11) correspond to equations (7) and (11) in the paper by Sozou & English.

The boundary conditions employed here mean that the present solution, besides its main interpretation, represents also the joint action of the agents generating the solutions constructed by Goldshtik and by Yih *et al.* for the case (in their notation) $T = 0$.

4. The Stokes flow problem

If a , b and k are such that the coefficient of u in (11) is small, then $u \approx 1$ and hence

$$\Omega \approx a + b(1-\mu), \quad (14)$$

$$\zeta \cdot r = \Gamma b/r. \quad (15)$$

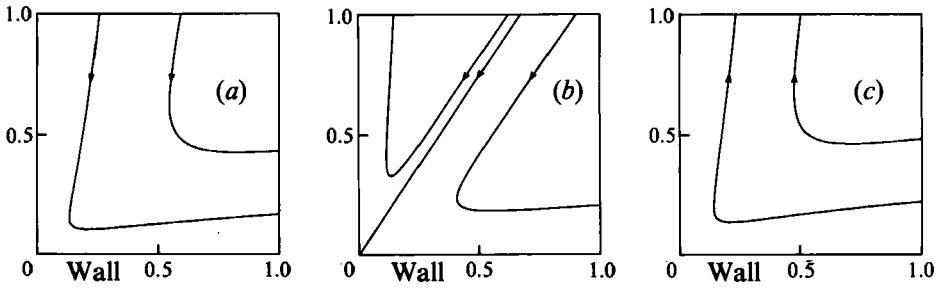


FIGURE 3. Schematic representation of meridional flow patterns for the Stokes flow regime. (a) $a = 0$ or 1 , $b > 0$ or $a = 1$, $b < -4.86$; (b) $a = 1$, $-4.86 < b < -2.70$; (c) $a = 1$, $-2.70 < b < 0$.

If we substitute (14) in (5) and, ignoring the nonlinear terms in g , integrate the resulting expression four times and apply the boundary conditions $g(0) = g'(0) = g(1) = 0$ we obtain

$$g = bk^2[a((1+\mu)^2 \ln(1+\mu) - (1-\mu)^2 \ln(1-\mu)) - 4(a+b)(1+\mu) \ln(1+\mu) + (2a+4b)((2 \ln 2 - 1)\mu^2 + \mu)]. \quad (16)$$

The derivation of (16) implies that, for this regime, the azimuthal flow and radial vorticity drive the poloidal flow and are not affected by it. When there is interaction between the poloidal and azimuthal flows the problem must be solved numerically. This is done in §5.

Equation (16) consists of two parts; one with coefficient abk^2 and one with coefficient b^2k^2 . Both parts are negative if a and b have the same sign. Therefore for all a and b , g has at most one zero.

If $a = 0$, $g(\mu) < 0$ and (16) represents a one-cell solution with down-draught in the axial region and radial outflow near the wall. This is the configuration for $R \ll 1$, $T = 0$ in the paper by Yih *et al.* Apart from a constant negative factor, the g -field is the same as that found by Lundquist for the corresponding MHD flow field mentioned before; the proportionality constant is negative because here the 'force' driving the flow is directed oppositely to the Lorentz force in the MHD problem.

If we change the signs of a and b we change the sign of Ω but g remains unaltered, and we shall assume that $a > 0$. A numerical evaluation of (16) revealed the following. (i) For $b > 0$, and also for $b < -(2 \ln 2 - 1)a/(3 \ln 2 - 2) = -4.86a$, $g(\mu) < 0$ and we have a one-cell flow configuration which has the same general direction as that associated with the case $a = 0$. (ii) For $-4.86a < b < -2.70a$, $g(\mu)$ changes sign; it is negative near the wall $\mu = 0$ and positive near the axis $\mu = 1$. The solution has a two-cell structure with radial outflow near the wall and an up-draught in the central region. (iii) For $0 > b > (2 - \ln 4)a/(4 \ln 2 - 3) = -2.70a$, $g(\mu) > 0$ and the flow field is a one-cell configuration representing an inflow near the wall and an up-draught in the central region. A schematic illustration of the flow pattern for the Stokes flow regime is shown in figure 3.

The flow for the case $b < 0$, $a + b > 0$, which relates to the configuration where the radial vorticity converges to the origin and is discharged in the axial direction and stretched, is similar to the one-cell flow pattern of figure 3(c). The stretching coefficient for this case may be defined by the positive quantity $\lambda = (a + b)/|b|$. It is evident from (14) that for a fixed b , Ω is larger when a , that is the stretching, is larger. Also it follows from (16) that for given $b < 0$ and k , g is larger when a is larger. These

observations mean that for a vorticity sink in a given fluid, that is for specified Γ , ν and b , both the azimuthal and poloidal flows are more intense for the case of larger stretching which is manifested as larger λ .

5. The nonlinear configuration

The basic parameters of the problem are ak and bk and we can fix one of the quantities a , b , k and solve the problem in terms of the other two. We set $a = 1$ and solved the problem for b and k . Since we are interested in the possible application of the solutions to atmospheric vortices, where the vorticity in the bulk of the fluid converges to the central region and is deflected in the axial direction where it probably undergoes intensification, we restricted the investigation of the nonlinear problem to the data $a = 1$, $-1 \leq b < 0$ and we refer to cases associated only with these data. The problem was solved iteratively as follows. We specified Ω and constructed $G(\mu)$ from (13) and then solved (11) by forward integration (Runge–Kutta methods) subject to $u(0) = 1$, $u'(0) = 0$. The function $u(\mu)$ was substituted in (12) for an improved approximation to Ω , which was used in (13) for a new $G(\mu)$ which was then used for a new $u(\mu)$ and so on until convergence. We assumed that convergence was achieved when the values of u and Ω (at all points) obtained at two successive approximations were the same to the fourth decimal place. For prescribed b we started the process by selecting a relatively low value of k , say k_1 , and setting $\Omega = 1 + b - b\mu$. When we constructed a solution we increased k from k_1 to k_2 and used the $\Omega(\mu)$ associated with k_1 as a start-off approximation for k_2 and the same b . This process was repeated for constructing a solution to a higher k , say k_3 , and so on. When k was close to a critical value the successive values of Ω and u obtained from successive iterations were oscillating. To overcome this difficulty we used under-relaxation for the Ω -values and eventually the relaxation parameter was set equal to zero. We used a step length of 0.0005. Some numerical experiments indicated that for the values of our parameters this step length yields reasonably accurate results.

The same results were also obtained by a shooting method similar to that employed by Goldshtik & Shtern. Equation (6) was integrated to yield

$$(1 - \mu^2)G'' + 2\mu G' - 2G + 2\Omega^2 = 2, \quad (17)$$

since $G(1) = G'(1) = 0$ and $\Omega(1) = 1$. For prescribed b and k we set $\Omega(0) = 1 + b$, $g(0) = 0$, $G(0) = 0$ and guessed $\Omega'(0) = b_1$, $G'(0) = c_1$ and integrated (4), (17) and (7) from $\mu = 0$ to $\mu = 1$ using Runge–Kutta methods. The terms b_1 and c_1 were varied iteratively so as to satisfy the conditions $G(1) = 0 = G'(1)$. The values of $G(1)$ and $G'(1)$ were projected from those at the previous four points by assuming that at $x = 1$ the fourth-order differences for G and G' are zero. Near the critical stage (see later) the shooting method required a step length of 0.00005 to yield the same overall accuracy as the previous procedure. Figure 4 shows the flow fields for $a = 1$, $b = -0.1$ relating to $k = 1, 5$ and 6.66 . These flow fields are typical for configurations associated with $a = 1$, $-1 < b < 0$. The case $k = 1$ in effect relates to the Stokes flow regime. This is readily seen from the shape – practically a straight line – of the corresponding Ω -curve shown in figure 4(d). As k increases so do the nonlinearities of the problem. The vorticity is convected towards the axis and the flow intensifies. The intensification of the flow is evident from figure 4(a–c). The convection of vorticity towards the axis is deduced from figure 4(d). The solid angle of a cone having as axis the line $\mu = 1$ and bounded by the generators $\mu = \mu_0$ is $2\pi(1 - \mu_0)$ and the radial vorticity input into the origin sink through the cone is $2\pi(\Omega(1) - \Omega(\mu_0))$.

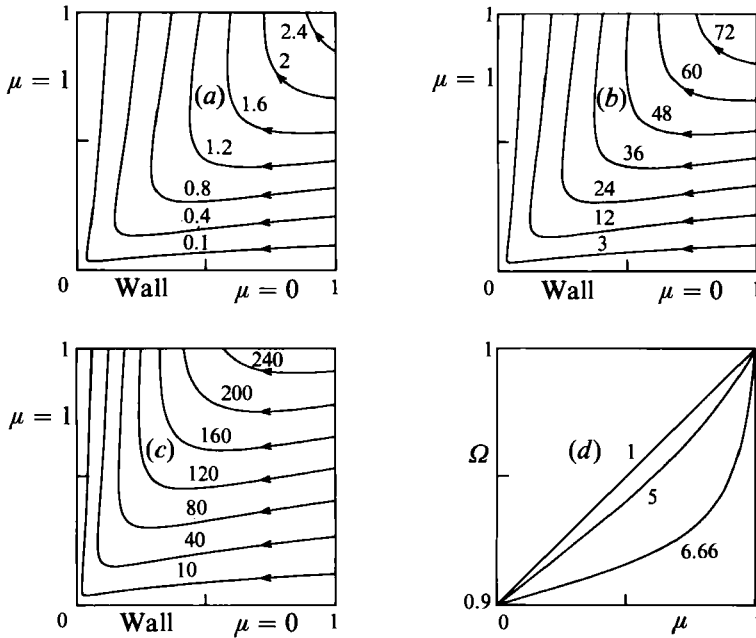


FIGURE 4. Streamlines in a meridian plane and values of Ω for $a = 1$, $b = -0.1$ and various k : (a) $k = 1$, (b) $k = 5$, (c) $k = 6.66$. In (a-c) the numbers on the curves are values of $100\psi/\nu L$, where L is a characteristic length. In (d), the corresponding Ω -curves, the numbers on the curves are values of k .

We find, for example, that the cone $\mu_0 = 0.8$ (whose solid angle is 20% of that of the hemisphere $\mu = 0$) for $k = 5$ and 6.66 contains 29 and 66%, respectively, of the radial vorticity of the system. (For $b = -0.1$ and $6.34 < k < 6.67$ there is another set of solutions (described later) where the radial vorticity is convected towards the axis and the velocity intensifies as k decreases.) For $k = 6.663$ (and $b = -0.1$) we constructed a solution yielding $u(1) = 0.146$ but for $k \geq 6.67$ neither the procedure involving (11)–(13) nor the shooting method produced a convergent solution. Clearly there is a critical value for k close to 6.67 . It actually turns out that there are two critical values of k associated with this problem.

The functions G , u' and u'' are negative and therefore as μ increases, u and u' decrease. We assume that for a fixed b as we vary k at or beyond some critical value, u vanishes at $\mu = 1$; that configuration represents velocity breakdown at $\mu = 1$. It is easily seen from (12) that if $u(1) \rightarrow 0$, then $\Omega \rightarrow 1 + b$ for $\mu < 1$.

It is a straightforward matter to show from (11) and (13) that if $\Omega = 1 + b$, then

$$u'' = -\frac{A}{(1-\mu^2)^2} \mu(1-\mu)u, \tag{18}$$

where $A = -k^2(2b + b^2)$. The conditions for the solution of (18) are $u(0) = 1$, $u'(0) = 0$, $u(1) = 0$ and $u > 0$ for $\mu < 1$. Equation (18) yields the limiting value $A = A_0 = 7.644$ that was mentioned in §3, from which we derive the smaller critical value for k , say k_{c1} given by

$$k_{c1} = 2.765/(-2b - b^2)^{\frac{1}{2}}. \tag{19}$$

For $b = -0.1$, (19) yields $k_{c1} = 6.343$. For $b = -0.1$ the other critical value of k , say k_{c2} , is close to 6.67 .

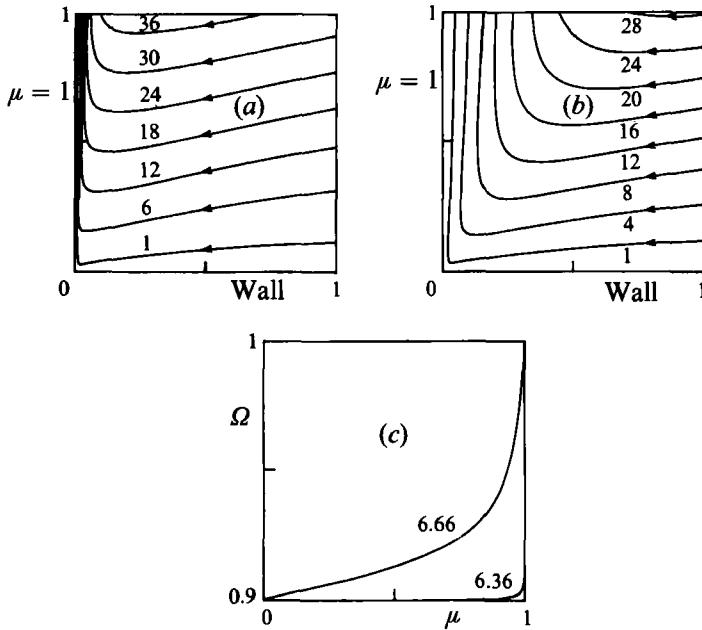


FIGURE 5. Streamlines in a meridian plane and values of Ω for type II solutions for $a = 1$, $b = -0.1$; (a) $k = 6.36$, (b) $k = 6.66$. In (a, b) the numbers of the curves are values of $10\psi/\nu L$, where L is a characteristic length and in the Ω -curves of (c) they are values of k . Note that the scaling of the streamlines in figures 4 and 5 differs by a factor of 10.

For a given k in the range $k_{c1} < k < k_{c2}$ there are two solutions to the problem. One of these represents the natural development of the solution as we gradually increase k through k_{c1} . We shall refer to this as a type I solution. The solution shown in figure 4(c) is such a solution. The other solution emanates from the limiting configuration associated with

$$\mu = 1, \quad \Omega = 1 + b, \quad k = k_{c1}.$$

Figure 5 shows two such solutions for $b = -0.1$. We shall call these solutions type II. When k is close to k_{c1} the flow has a jet-like structure with all the radial vorticity concentrated in a thin cone about the axis of the system and the circulation about the axis is $2\pi\Gamma(a + b)$, a constant. Such a configuration is shown in figure 5(a) which relates to $k = 6.36$. As k increases, the intensity of the flow decreases and the radial vorticity of the type II solution spreads. This is evident by comparing the flow fields shown in figures 5(a) and 5(b) and the Ω -curves of figure 5(c). Our detailed data show that for $k = 6.36$ and 6.66 the cone bounded by the generators $\mu = 0.8$ contains 99.5 and 72% of the radial vorticity of the system. It is impossible to calculate k_{c2} exactly, but our computations show that at k_{c2} the types I and II solutions coalesce. A similar situation can arise in the problem considered by Serrin. According to Goldshtik & Shtern (1990, p. 495), for a region of the parameter space used by Serrin there are two regular solutions which on a section of the boundary ‘merge and disappear’. These authors suggest (private communication) that the same situation arises in the present problem, and for $k > k_{c2}$ the velocity develops a singularity along the axis of the system. Their reasons are given in the Appendix.

Table 1 shows values of k_{c1} and approximate values of k_{c2} for some values of b .

The approximate values of k_{c2} shown in table 1 are slightly larger than those associated with coalescence and relate to velocity breakdown. For $b = -1$, that is for

b	k_{c1}	k_{c2}
-1	2.765	2.765
-0.5	3.193	3.27
-0.1	6.364	6.67
-0.002	43.74	46.3

TABLE 1. Values of k_{c1} and approximate (which are slightly larger than) values of k_{c2} for some values of b .

the case investigated by Goldshtik, there are no type II solutions and when the value of k is close to (but less than) 2.765 the poloidal flow has a jet-like structure similar to that shown in figure 5(a). Inspection of table 1 shows that as $|b|$ decreases, the gap between the two critical values of k increases slowly.

The numerical programming, computations and the organization of the diagrams of this paper were carried out by Mark Ashton and Linda Wilkinson.

Appendix. The solution for $k > k_{c2}$

By M. A. Goldshtik and V. N. Shtern

Institute of Thermophysics, Novosibirsk 630090, Russia

To investigate how the solution of the problem breaks down for $k > k_{c2}$ we consider the solution of (4), (6), and (7) in the region $0 \leq \mu \leq \mu_0 \leq 1$, where μ_0 is close to 1, subject to the following boundary conditions:

$$\text{at } \mu = 0, \quad g = g' = 0, \quad \Omega = 1 + b; \quad (\text{A } 1)$$

$$\text{at } \mu = \mu_0, \quad g = G' = 0, \quad \Omega = 1. \quad (\text{A } 2)$$

We note, from differentiating (7) and using (A 2), that $g''(\mu_0) = 0$. For given b and k we set $g(0) = g'(0) = G(0) = 0$, $\Omega(0) = 1 + b$ and prescribed $\Omega'(0) = b_1$, $G'(0) = c_1$ and $G''(0) = c_2$ and integrated (4), (6) and (7) from $\mu = 0$ to $\mu = \mu_0$. The parameters b_1 , c_1 and c_2 were varied iteratively until the conditions (A 2) were satisfied. In figure 6 we plot the parameter b_1 for some values of k . The solid curve refers to the exact solution. The branches yielding solutions types I and II are labelled accordingly. The broken curve refers to the modified solution for the region $0 \leq \mu \leq \mu_0 = 0.999$ and has three branches. The first branch is close to branch I, the second branch is close to branch II and the third branch is almost parallel to the k -axis and stretches to $k = \infty$. For given k , values of b_1 associated with the first and second branches yield solutions similar to types I and II, respectively. Values of b_1 associated with the third branch yield solutions that have a jet-like structure near μ_0 . As $\mu_0 \rightarrow 1$, the first and second branches of the broken curve tend to branches I and II, respectively, of the solid curve. The third branch tends to the k -axis, and at μ_0 the absolute value of $g'(\mu_0)$ associated with this branch increases very rapidly. Since for $k > k_{c2}$ only the third branch exists, it means that for $k > k_{c2}$ and $\mu_0 \rightarrow 1$ the velocity field develops a singularity on the axis and breaks down there. Note that in that case the azimuthal friction $\Omega'(0) = b_1$ vanishes.

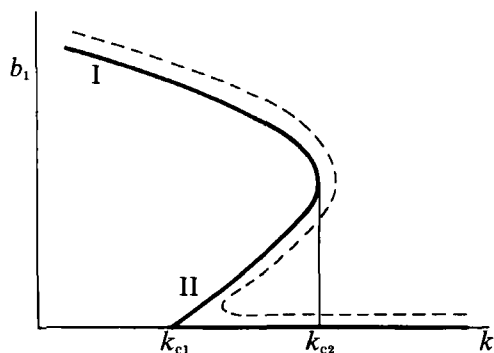


FIGURE 6. Values of $b_1 = \Omega'(0)$ in terms of the parameter k . The solid curve represents the exact solution. The numbers I and II show the b_1 values that yield types I and II solutions. The broken curve relates to the modified solution for $\mu_0 = 0.999$.

REFERENCES

- GOLDSHTIK, M. A. 1960 *J. Appl. Math. Mech.* **24**, 913–929.
 GOLDSHTIK, M. A. & SHTERN, V. N. 1990 *J. Fluid Mech.* **218**, 483–508.
 LIGHTHILL, M. J. 1963 In *Laminar Boundary Layers* (ed. L. Rosenhead), p. 50. Oxford University Press.
 LUNDQUIST, S. 1969 *Ark. Fys.* **40**, 89–95.
 MAXWORTHY, T. 1973 *J. Atmos. Sci.* **30**, 1717–1722.
 PAULL, R. & PILLOW, A. F. 1985a *J. Fluid Mech.* **155**, 343–358.
 PAULL, R. & PILLOW, A. F. 1985b *J. Fluid Mech.* **155**, 359–379.
 SERRIN, J. 1972 *Phil. Trans. R. Soc. Lond. A* **271**, 325–360.
 SHIVOLA, E. I. & SHCHERBININ, E. 1971 *Magnetohydrodyn.* **7**, 167–171 (English transl.).
 SIMPSON, J. 1982 In *Intense atmospheric vortices* (ed. L. Bengtsson & J. Lighthill), pp. 161–173. Springer.
 SIMPSON, J., MORTON, B. R., McCUMBER, M. C. & PENC, R. S. 1986 *J. Atmos. Sci.* **43**, 753–782.
 SNOW, J. T. 1984 *Sci. Am.* **250** (4), 56–66.
 SOZOU, C. 1971 *J. Fluid Mech.* **46**, 25–32.
 SOZOU, C. & ENGLISH, H. 1972 *Proc. R. Soc. Lond. A* **329**, 71–82.
 SQUIRE, H. B. 1952 *Phil. Mag.* **43** (7), 942–945.
 YIH, C. S., WU, F., GARG, A. K. & LEIBOVICH, S. 1982 *Phys. Fluids* **25**, 2147–2158.